

Article

Influence of Surface Preparation Method on the Bond Behavior of Externally Bonded CFRP Reinforcements in Concrete

Sérgio Soares, José Sena-Cruz *, José Ricardo Cruz and Pedro Fernandes

Institute for Sustainability and Innovation in Structural Engineering (ISISE), Department of Civil Engineering, University of Minho, Azurém Campus, 4800-058 Guimarães, Portugal; a65181@alunos.uminho.pt (S.S.); a51314@alunos.uminho.pt (J.R.C.); pmgfernandes@outlook.com (P.F.)

* Correspondence: jsena@civil.uminho.pt; Tel.: +351-253-510-200

Received: 18 November 2018; Accepted: 28 January 2019; Published: 29 January 2019



Abstract: In last decades significant investigation has been carried out in order to predict the bond strength of externally bonded reinforcement (EBR) systems with carbon fiber reinforced polymer (CFRP) materials in concrete and, as consequence of that, many analytical expressions can be found in the literature, including in standards. However, these expressions do not account for the influence of several parameters on bond behavior such as the type of surface preparation which is a mandatory and critical task in the strengthening application. The present work gives contributions to reduce this lack of knowledge. For this purpose, an experimental program composed of single-lap shear tests was carried out, the main parameters studied being: (i) the type of concrete surface preparation (i.e., grinding and sandblasting) and (ii) the bond length. Prior to the application of the EBR CFRP system, the roughness level provided by the different methods of surface preparation was characterized by a laser sensor. Test results revealed that sandblasting concrete surface preparation yielded higher values, in terms of maximum shear force and fracture energy. Finally, existing expressions in standards were upgraded in order to account for the concrete surface roughness level in the estimation of the bond strength.

Keywords: EBR; CFRP laminates; concrete surface preparation; roughness characterization; bond behavior; analytical predictions

1. Introduction

In last decades, fiber reinforced polymer (FRP) materials have been increasingly proposed to strengthen reinforced concrete (RC) structures [1–3]. This approach has been demonstrated as an effective alternative solution to the traditional strengthening methods which typically employ reinforced concrete and/or steel. FRP materials have shown to be a useful and efficient solution due to their good mechanical properties, lightness, resistance to corrosion, low thermal conductivity, good fatigue behavior and easy installation procedures [4,5]. Different strengthening techniques have been developed for applying FRP. The first one, Externally Bonded Reinforcement (EBR), appeared in the 1980s [6,7], where the FRP laminate is glued onto the tensile face of the RC element. A few years later, other techniques emerged such as the near-surface mounted (NSM), where the FRP laminate or bar is inserted onto a groove previously cut in the concrete cover. According to the literature, when FRP are used as reinforcement material, bond behavior between this and concrete substrate is generally a critical issue for both EBR [8–19] and NSM techniques [13,16,20–24] that directly influence the effectiveness of the structural reinforcement. The strengthening performance of these techniques depends significantly on the resistance of the concrete cover, which is normally

the most degraded concrete region in the structure and the concrete surface condition. As a result, premature failure of FRP reinforcement can occur and, generally, its full mechanical capacity is not mobilized, mainly when adopting the EBR technique. In attempt to overcome these issues, other strengthening techniques with composite materials have emerged such as Mechanically Fastened and Externally Bonded Reinforcement (MF-EBR) [4,25], which uses multi-directional carbon fiber laminates, simultaneously glued and anchored to concrete, and Mechanically Fastened FRP (MF-FRP) [25–29] using only steel anchors to fix the laminate to the substrate. Despite their potential, these techniques also reveal some shortcomings such as (i) the possible concrete damage during anchoring, (ii) the limited opportunity of anchor's installation in the presence of congested internal reinforcement in the members to be strengthened and (iii) other problems related to the stress concentration and bearing failures of the systems leading to slippage of FRP and loss of bond.

The present work focuses on the bond behavior characterization between EBR CFRP system reinforcement and the concrete surface. As many researchers verified in their experimental works when this technique was applied, the bond strength depends on several factors, including mechanical and physical properties of concrete, composite material and epoxy adhesive which prevent the fully FRP tensile strength to be attained due to the premature debonding failure that typically occurs [12,13,15]. Moreover, it is well known that the concrete surface preparation and bonding technique are crucial tasks for adequate installation of an EBR FRP system to delay the brittle debonding failure. Therefore, it is a key issue to proceed a preparation method that ensures the cleanliness, the soundness and a proper concrete surface roughness level [11,12]. More specifically, the concrete surface preparation process includes the removal of unsound concrete, strength verification and opening of the pore structure. The methods that have been most used by the scientific community are sandblasting, grinding, brushing, scarifying, steel shot blasting and bush hammering with different advantages and disadvantages associated, in terms of roughness level provided, cost, processing time and application difficulties. Through bond characterization tests between concrete surface and FRP, some authors demonstrated that the bond strength is higher when an effective surface preparation method is used due to the higher surface roughness level that provides better adhesion along the system interface [11,12,18,19].

In terms of standard guidelines, the influence of the concrete surface roughness on the EBR system performance and bond strength has been recognized in a comprehensive manner [1,2,30,31]. According to the International Federation for Structural Concrete (fib) [2], the concrete substrate should be roughened and made laitance and contamination free, in such a way that the concrete quality can be utilized in an optimum way. This guideline recommends that the surface preparation is done preferably by means of high-pressure blasting (sand, grit, water jet blasting) or grinding. In turn, the ACI Committee 440 [31] proposes that at least the application of abrasive or water blasting techniques for surface preparation should be performed. On the other hand, the Italian National Research Council [1] highlights the importance of a quality control that includes the determination of concrete conditions, removal of any deteriorated or loose concrete, cleaning and protection from corrosion of existing steel reinforcement, and finally substrate preparation for receiving the selected FRP reinforcement. In accordance with this standard, once the quality control of the substrate had been performed, the deteriorated concrete had been removed, the concrete cross section had been restored, and the existing steel reinforcement had been properly treated, sandblasting of the concrete surface shall be performed.

Although the main guidelines recognize that concrete surface preparation prior the installation of the EBR FRP is an important task, the analytical formulations provided to predict the system bond strength still do not consider the influence of the use of different methodologies to do that. Possible reasons for this reside on the fact that different concrete preparation methods provide different roughness levels of the surface. Additionally, sometimes it is difficult to obtain a uniform surface roughness level, because this depends on human skills in the execution of the surface preparation method and it becomes a critical aspect when specimens under the same test conditions are produced. Therefore, a good scientific development would be to quantify the roughness level of the concrete

surface before the reinforcement procedure and to understand how this influences the bond behavior of the EBR FRP system, when different methodologies of surface preparation are used. Then, the next step would be to introduce this influence on the bond strength prediction formulations. To measure the concrete surface roughness level after the application of different methods of surface preparation, several authors have used lasers profilometers [11,32,33]. This approach has proven to be very effective for quantifying the roughness level of the concrete surface, and can be the key to correlating this result with the bond behavior of the strengthening system. The use of this technology is something that is feasible in fieldwork, namely in a real application of the EBR FRP system. Nowadays, there are already commercial and patented systems that allow the assessment of the quality control of the concrete surface preparation. Thus, concrete surface roughness should be a requirement at the execution stage of the intervention and subject to quality control before proceeding to the concrete element strengthening.

The present paper aims at contributing to a better understanding the influence of the use of different concrete surface preparation methodologies on the bond behavior of CFRP EBR systems. For this purpose, an experimental program composed of single-lap shear tests was carried out. This was performed by adopting an experimental set-up developed by the authors and the main parameters studied were the type of concrete surface preparation (SB—sandblasting and GR—grinding) and the bond length between CFRP and concrete surface. Prior to the application of the EBR CFRP system, the roughness level provided by the different methods of surface preparation was characterized by a laser sensor, in order to make it possible to correlate these measurements with the results obtained in the bond tests which characterize the interface behavior between concrete and CFRP laminate. Then, the formulation proposed by the Italian National Research Council [1] was updated in order to account for the roughness level of the concrete surface on the estimation of the bond strength.

2. Experimental Program

2.1. Test Program

The main objective of the present investigation was to characterize the bond behavior of concrete elements with EBR CFRP systems, considering the following study variables: (i) the concrete surface preparation method and (ii) the bond length. The program was composed of 24 single-lap shear tests divided into two main groups according to the concrete surface preparation methodology used: (i) GR—grinding and (ii) SB—sandblasting. The selection of these two methods of concrete surface preparation was based on the fact that these two have been the most used in structural strengthening with the EBR technique. In each group, three different bond lengths (L_b) were considered: (i) 150 mm, (ii) 200 mm and (iii) 250 mm. According to some provided analytical formulations [1,2,8], the theoretical value of the effective bond length ranges between 191 and 217 mm. This means that the L_b values adopted represent, respectively, a lower, an approximate, and a higher value than the theoretical effective bond length. Thus, it is possible to perform an analysis of the influence of the L_b adopted on the EBR CFRP system bond behavior. Consequently, six series were adopted, each one composed of four specimens in the same conditions in order to ensure reliable results. The generic denomination of the test specimens is X_LbY_Z, where X represents the concrete surface preparation method (GR or SB), Y is the bond length in millimetres (150, 200 or 250) and Z is the specimen order number tested under the same conditions (1, 2, 3 or 4).

2.2. Specimen's Geometry, Experimental Set-Up and Instrumentation

Figure 1 depicts the test set-up and instrumentation adopted in the experimental program for the case the specimen with a L_b of 200 mm. Concrete blocks of $400 \times 200 \times 200 \text{ mm}^3$ were used, where two CFRP laminate strips were applied in opposite faces (parallel to the casting direction), according to the EBR technique. Pultruded CFRP laminate strips with 50 mm of width and 1.2 mm of thickness were used. To avoid premature failure by concrete rip off ahead of the loaded end, the bonded lengths

started 100 mm apart, from the extremity. The concrete specimen was placed horizontally on a steel plate (support S1) with 70, 300 and 550 mm of thickness, width and length, respectively. Support S1 was fixed to the stiff base of the testing steel frame system through eight M16 steel threaded rods. To assure negligible horizontal displacements of the concrete block in the loading direction during the test, a steel plate (support S2) was placed in the bottom front part of the concrete block, which acted as a reaction element at a height of 50 mm. To minimize vertical displacements during the test, a steel plate (support S3) of $50 \times 70 \times 300 \text{ mm}^3$ was placed in the rear top part of the concrete block. Both support S2 and S3 were fixed to the support S1 through two M20 steel threaded rods. The tests were performed using a servo-controlled equipment (INEGI, Porto, Portugal). The applied force was measured through a load cell of 200 kN maximum carrying capacity (linearity error of 0.05% F.S.), placed between the actuator and the grip used to fix the CFRP laminate during the test. The relative displacement between the CFRP and the concrete (slip) at the loaded end section (s_l) was computed as the average of displacements measured by the linear variable displacement transducers (LVDT) 1 and 2 with a stroke of $\pm 5 \text{ mm}$ (linearity error of 0.24% F.S.). The tests were performed under displacement control at the loaded end through LVDT2 (rate of $2 \mu\text{m/s}$). Additionally, a series of four strain gauges TML BFLA-5-3-3L (SG1 to SG4) were placed along the CFRP laminate centerline to measure the longitudinal strains during the loading process (Figure 1).

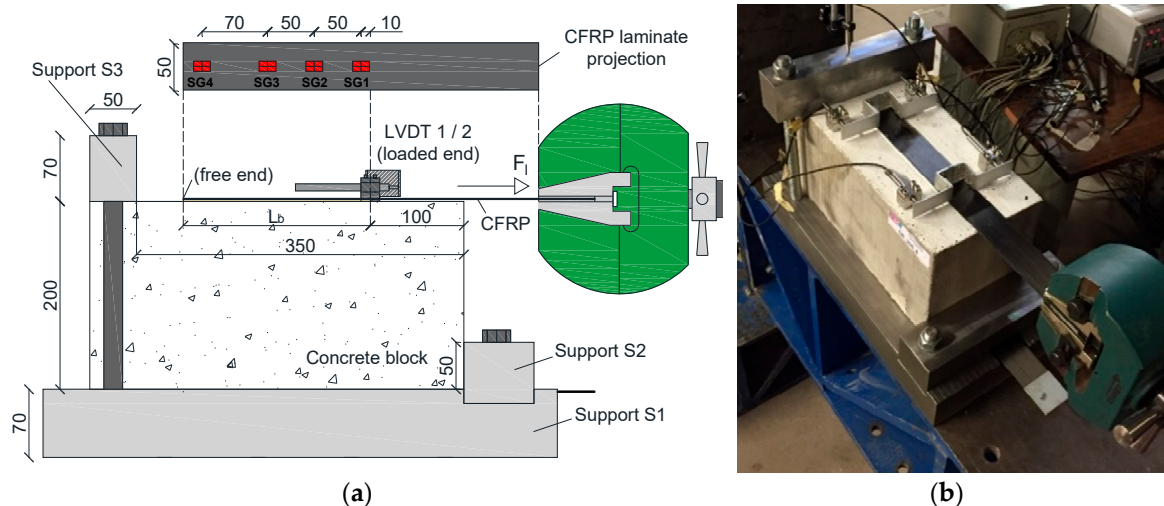


Figure 1. Experimental set-up and instrumentation: (a) scheme; (b) photo. Note: units in [mm].

2.3. Specimen's Preparation

According to the test program, two different methods of concrete surface preparation were studied. The surface preparation consists of removing the superficial concrete layer with inappropriate characteristics in order to obtain a clean and healthy surface with absence of the laitance layer and with an adequate roughness level, showing the aggregates. The aim was to understand the influence of the different methodologies in terms of providing concrete surface roughness and its consequence on the bond behavior of the EBR system. The two concrete surface preparation methods used in the experimental program are presented in Figure 2: (i) GR—grinding and (ii) SB—sandblasting. Both surface preparation methods used are relatively easy to apply. The GR is a mechanical method of surface preparation and consists of removing the unsound concrete layer through rotating shafts with sprockets that progressively wear out the surface layer. In this case, a grinding wheel was used until the aggregates had become visible (see Figure 2a). In turn, SB is a process of surface preparation based on particles' impacts, being one of the most used techniques. This consists of the projection of small particles against the surface in order to cause surface abrasion and wear due to the high speed of projection (see Figure 2b), allowing a faster concrete surface preparation than the GR method. However, the SB method application requires professional equipment and skilled labor. After surface

preparation, the treated surface was cleaned by high-pressure water jet (Figure 2c) to remove the debris and dust resulting from the treatment applied, ensuring a good adhesion between the concrete surface and the reinforcing system. The next steps of preparing the specimens were performed after the specimens became dry.



Figure 2. Concrete surface preparation: (a) grinding; (b) sandblasting; (c) surface cleaning.

2.4. Concrete Surface Roughness Characterization

Considering the different preparation methodologies of the concrete surface (GR and SB), the roughness of these distinct surfaces was measured and analyzed. The main purpose was to relate the different methodologies to the provided concrete surface roughness and with the bond between CFRP laminate and concrete substrate. The procedure involved the use of a laser sensor, whose main characteristics are presented in Table 1. Three longitudinal profiles (with 20 mm apart from each other—transverse direction) were analyzed by the laser sensor in each of the 24 surface areas where the EBR CFRP system was installed. The roughness measurement through the laser sensor allowed to obtain qualitative and quantitative information of the different surfaces. The configuration of the surface roughness measuring system is also stated in Table 1. The laser sensor was connected to a metallic plate, which was part of a mechanism conceived to produce a slow displacement at a constant rate, as well as to allow the displacement of the laser sensor during scanning at a parallel and rectilinear path relatively to the scanned surface. The displacement rate was 8.8 mm/s and the data acquisition rate was 34 Hz, leading to consecutive readings spaced at 0.3 mm. Representative roughness profiles provided by the two methods of surface preparation and obtained by the laser sensor along 50 mm of the bonded length are shown in Figure 3. The results clearly show that the SB method produced a higher level of surface roughness than the GR method.

Table 1. Properties of laser sensor SICK OD2—N50W10U0 and roughness measurement system.

Parameter	Value	Roughness Measurement System
Measuring range	40 to 60 mm	
Resolution	5 μm	
Repeatability	15 μm	
Measuring frequency	2 kHz	
Light spot dimension (distance)	0.5 mm × 1 mm (50 mm)	

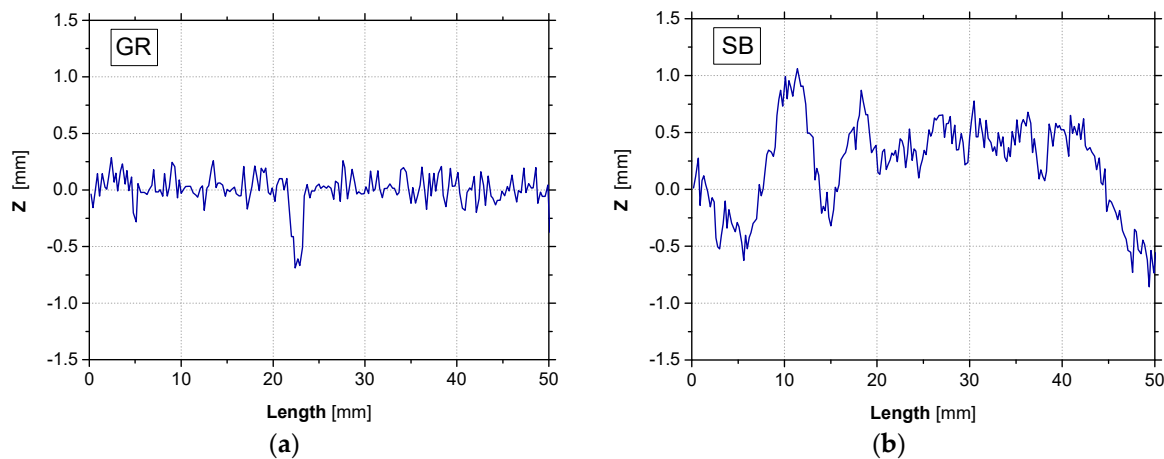


Figure 3. Roughness profile when different surface preparation methods were applied: (a) grinding; (b) sandblasting.

To quantitatively characterize the roughness level provided by each of the surface preparation methods several statistical indicators were considered, such as the mean roughness coefficient (R_m) and the root mean square (R_q). These indicators can be determined using Equations (1) and (3), respectively. In these equations, the parameters l , $z(x)$ and n are the evaluation length, the profile height at position x and the number of scan readings performed by the laser sensor, respectively.

$$R_m = \frac{1}{l} \int_0^l |z(x) - \bar{z}| \cdot dx \approx \frac{1}{n} \sum_{i=1}^n |z_i - \bar{z}|, \quad (1)$$

$$\bar{z} = \frac{1}{l} \int_0^l z(x) \cdot dx \approx \frac{1}{n} \sum_{i=1}^n z(x), \quad (2)$$

$$R_q = \sqrt{\frac{1}{n} \sum_{i=1}^n z_i^2}. \quad (3)$$

The statistical indicators used were then computed for the two different types of surface preparation and the results from the roughness assessment are presented in Table 2. The comparison between the value of the parameters R_m and R_q provided by each surface preparation method is established in the Figure 4.

Table 2. Results from the roughness assessment (average values).

Series	Roughness Parameter [mm]	
	Mean Roughness Coefficient (Absolute Value), R_m	Root Mean Square, R_q
GR_Lb150	0.137 (21.8%)	0.260 (32.7%)
GR_Lb200	0.120 (10.3%)	0.181 (11.5%)
GR_Lb250	0.165 (13.4%)	0.329 (29.4%)
Mean value	0.141	0.256
SB_Lb150	0.533 (17.9%)	0.655 (21.8%)
SB_Lb200	0.460 (14.8%)	0.570 (9.4%)
SB_Lb250	0.491 (31.1%)	0.691 (32.7%)
Mean value	0.494	0.639

Notes: the values in parentheses are coefficients of variation (CoV).

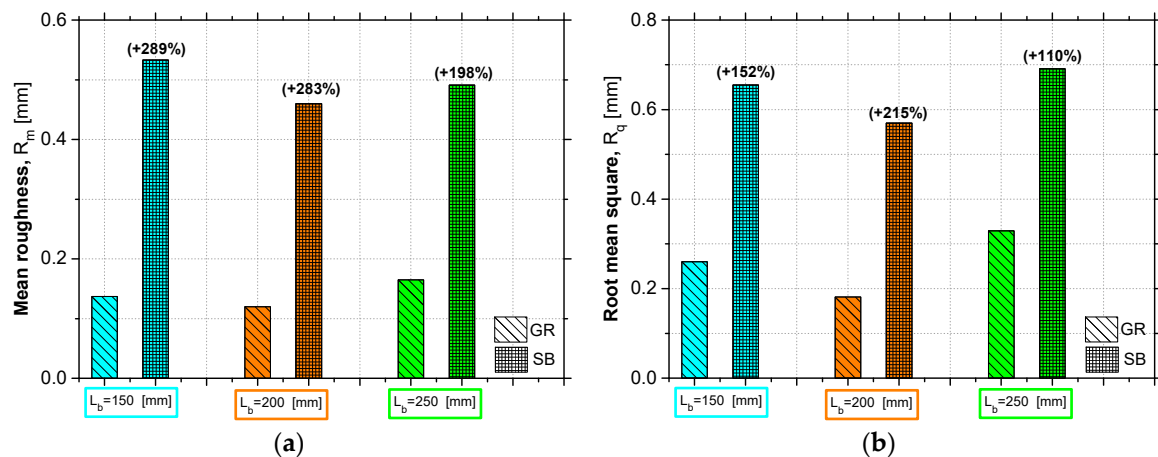


Figure 4. Roughness level comparison provided by each surface preparation method (GR and SB) in terms of: (a) mean roughness (R_m); (b) root mean square (R_q). Note: the values in parentheses represents the percentage increase when SB was applied instead of GR.

The results of each statistical indicator were obtained by the average value of the four test specimens with the same test conditions, i.e., the specimens with the same bond length and the same concrete surface type. According to the results, it is possible to verify that the SB method allowed to obtain considerably higher roughness levels than the GR. In terms of R_m and R_q , the SB method allowed an average increase of 250% and 150%, respectively, in relation to the surface preparation with GR. It is important to note that the values of coefficient of variation (CoV) are sometimes significant due to the difficulty of obtaining a uniform surface roughness level. This depends on the human skill in the execution of the surface preparation method, as well as on the homogeneity of the material, and becomes a critical aspect when specimens under the same test conditions are produced, in which, theoretically, the same levels of roughness would be desired.

2.5. Material Characterization

The material characterization included the assessment of the mechanical properties of the materials involved in this experimental program, mainly: (i) concrete, (ii) CFRP laminate strip and (iii) epoxy adhesive. Table 3 shows the obtained results.

Only one batch was used for casting all the test specimens. The used concrete had the following characteristics: class C25/30; exposure class XC2; maximum aggregate size of 12.5 mm; slump S4. The average Young's modulus (E_{cm}) and average compressive strength of concrete (f_{cm}) were assessed using five cylinders with 300 mm of height and 150 mm of diameter and following the recommendations NP EN 12390-13:2014 [34] and NP EN 12390-3:2011 [35], respectively, at 28 days of concrete age.

The CFRP laminate strips used in the experimental work (type: S&P Laminates CFK) consists of unidirectional carbon fibers held together by an epoxy vinyl ester resin matrix. These were produced by S&P® Clever and Reinforcement with the trademark CFK 150/2000. According to the manufacturer, this type of CFRP laminate presents a smooth external surface and the fiber volume content is about 70%. Pultruded CFRP laminate strips with 50 mm of width and 1.2 mm of thickness were used. The tensile mechanical properties included the average Young's modulus (E_f), the average tensile strength (f_{fu}) and the average strain at the peak stress (ϵ_{fu}) were assessed using five samples and following the recommendation ISO 527-5:2009 [36].

The epoxy adhesive (type: S&P Resin 220 epoxy adhesive), produced by the same supplier as for the CFRP laminate, was used as bond agent to fix the reinforcing material to the concrete substrate. This adhesive is available in the form of two components (Component A—resin and Component B—hardener) that need to be mixed. According to the manufacturer, the ratio A:B in the mix should be 4:1. In the scope of the present experimental work, the epoxy adhesive was not characterized, and its

mechanical properties were collected from a previous work performed by some of the authors of the present work [21]. In this context, six samples were prepared and tested following the recommendation ISO 527-2:2012 [37]. These results are also presented in Table 3, in terms of average tensile strength (f_a), average Young's modulus (E_a) and average strain at the peak stress (ϵ_a).

Table 3. Material characterization (average values).

Concrete			
Age of curing	f_{cm} (MPa)	E_{cm} (GPa)	
28 days	33.4 (4.33%)	30.8 (2.84%)	
CFRP			
Cross-section geometry (mm ²)	f_{fu} (MPa)	E_f (GPa)	ϵ_{fu} (%)
50 × 1.2	2222.4 (4.7%)	176.4 (2.0%)	1.2 (2.2%)
Adhesive			
Type of adhesive	f_a (MPa)	E_a (GPa)	ϵ_a (%)
S&P Resin 220 epoxy adhesive ^a	22.0 (4.5%)	7.2 (3.7%)	0.36 (15.2%)

Notes: the values in parentheses are coefficients of variation (CoV); ^a Results collected from [21].

3. Results and Discussion

3.1. Main Results

In this section the main results obtained in the single-lap shear tests are presented. Table 4 summarizes the average results for each series obtained in the experimental program through several parameters that characterize the bond behavior between the CFRP and the concrete, mainly: $F_{l,max}$ is the maximum shear force; $s_{l,max}$ is the loaded end slip at $F_{l,max}$; G_f is the total energy up to 0.3 mm of loaded end slip (common s_l value attained in all the tests); ϵ_{fmax} is the CFRP normal strain at $F_{l,max}$; and, finally, FM represents the failure mode observed in each specimen tested.

Table 4. Main results obtained from the single-lap shear tests (average values).

Series	$F_{l,max}$ (kN)	$s_{l,max}$ (mm)	G_f (kN·mm)	ϵ_{fmax} (%)	FM
GR_Lb150	23.8 (6.9%)	0.34 (11.7%)	5.08 (5.4%)	0.22	D [4]
GR_Lb200	23.8 (4.7%)	0.34 (18.0%)	5.37 (6.6%)	0.22	D [4]
GR_Lb250	26.8 (7.9%)	0.35 (19.2%)	5.89 (6.2%)	0.25	D [4]
SB_Lb150	27.2 (6.7%)	0.31 (12.5%)	5.79 (3.0%)	0.26	D [4]
SB_Lb200	30.2 (9.7%)	0.41 (8.2%)	5.92 (3.7%)	0.29	D [4]
SB_Lb250	31.3 (5.7%)	0.52 (24.0%)	6.07 (2.9%)	0.30	D [4]

Notes: the values in parentheses are coefficients of variation (CoV); D = cohesive debonding in the concrete; the values between brackets [] are the number of specimens with the specified failure mode.

From a general analysis, a significant influence of the surface preparation method used on the bond behavior is verified. In fact, the SB method proved to be more efficient than GR because it allowed an increase in the bond strength against debonding failure. Therefore, when the same bond length was adopted, the SB method provided an increase of $F_{l,max}$, $s_{l,max}$, and G_f in relation to the GR method. In turn, the L_b adopted also showed to have influence on the bond behavior. With the

increase of L_b , a bond strength increase was observed, translated by the increase of the necessary shear force to induce debonding failure of the EBR system. Furthermore, when the same surface preparation method was used, the increase of L_b provided an increase of $s_{l,max}$ and G_f . In all tests, the debonding of the CFRP laminates occurred with a thin layer of concrete.

The shear force vs. loaded end slip curves (F_l-s_l) obtained in all tests carried out in this experimental work are presented in Figure 5. In each graph, the responses corresponding to the four specimens tested under the same conditions are gathered. Later, a more detailed analysis about the influence of the study variables is performed.

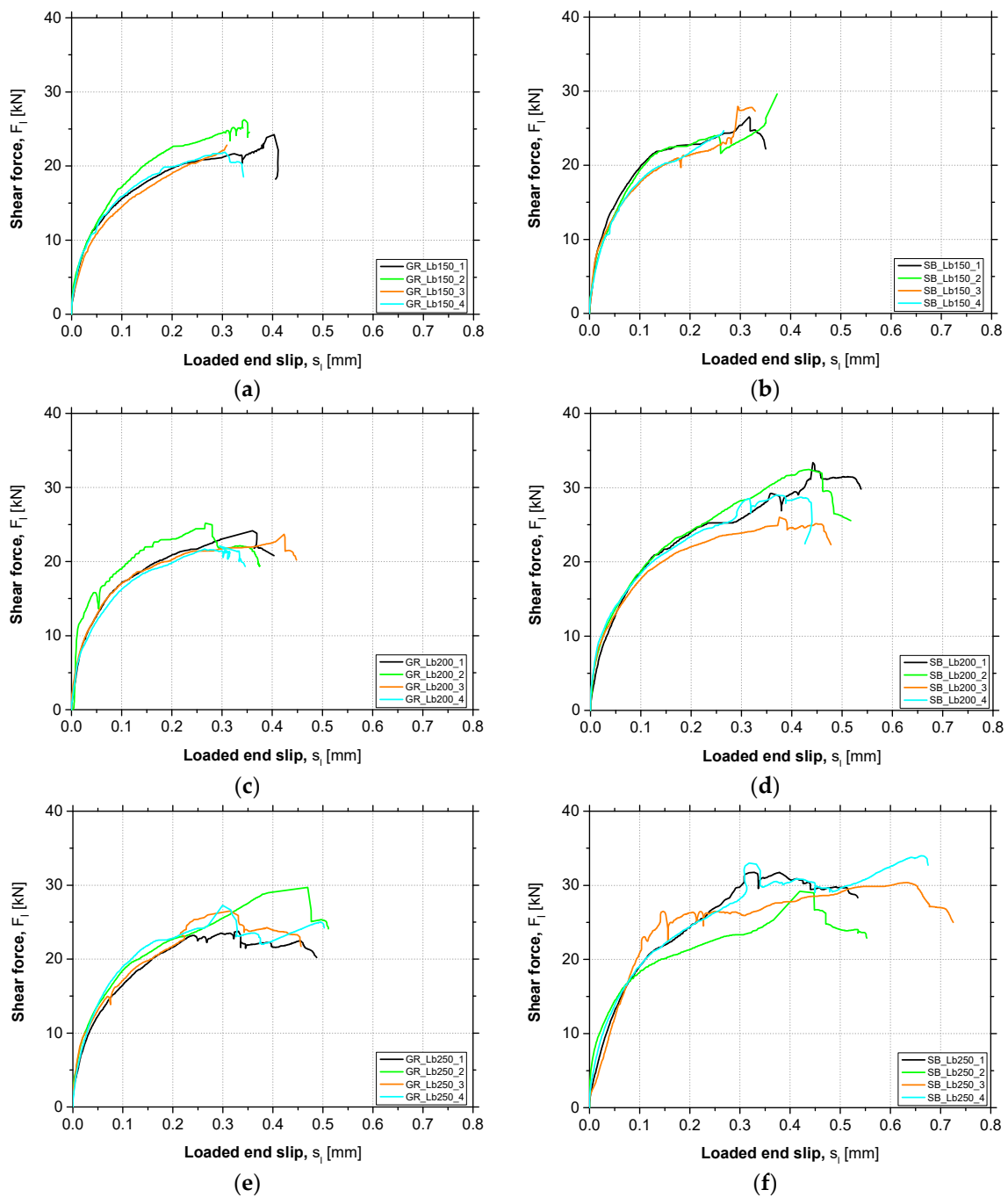


Figure 5. Shear force vs. loaded end slip obtained in each series: (a) GR_Lb150; (b) SB_Lb150; (c) GR_Lb200; (d) SB_Lb200; (e) GR_Lb250; (f) SB_Lb250.

In each F_l-s_l presented in the Figure 5, the three distinct phases in the behavior are observed regardless of the surface preparation method used and L_b adopted. The initial branch is almost linear, due to the behavior of the involved materials and perfect bond. After this phase, an increasing stiffness degradation can be observed due to the start of EBR CFRP bond degradation conditions. Then, an almost steady state phase can be observed, due to the debonding process. This process of failure starts when the ultimate shear strength is attained at the beginning of the bonded length, i.e., at the loaded end. During debonding failure, an increase in the loaded end slip at an almost constant value of applied shear force is observed. However, in some particular cases, after the initiation of the debonding process, a slight increase in the applied force was observed. This fact can be justified by possible heterogeneities in the concrete specimens, namely when the concrete layer, where failure occurs, crosses a coarse aggregate. This implies that a higher shear force would be required to increase the slip (friction at interface level). According to the responses presented in Figure 5, it is also important to highlight that the adopted test methodology proved to be adequate in providing a stable debonding process. Similar responses in terms of F_l-s_l curves have been obtained in other research studies, e.g., [12] or [13].

3.2. Failure Modes

As shown in Table 4, cohesive debonding in the concrete failure mode was observed in all the single-lap shear tests carried out, regardless of the surface preparation method used and bond length adopted. After debonding failure, a concrete layer attached to the epoxy adhesive and CFRP laminate was analyzed. This failure mechanism was also verified in others investigation works, e.g., [11,12].

During the loading process, inclined microcracks arose on the external concrete layer since the concrete tensile strength is lower than the corresponding adhesive's strength. The emergence of these microcracks occurred from the loaded end to the free end section, accompanying the debonding process of the EBR CFRP system that starts when the bond strength is reached. Therefore, the bond strength is gradually lost in the successive loaded end sections during the loading process, and then other zones of bonded length are activated, providing its contribution to the stress transfer. While the debonding failure occurs, the stress distribution capacity in the successive loaded end sections become nil. The characteristics of the failure mechanism observed highlight the importance of the adhesive properties and the use of an effective surface preparation prior the installation of the EBR CFRP system that promotes a good adhesion between the concrete surface and the reinforcing material. These are crucial aspects in order to make it possible to increase the bond strength against debonding failure. Therefore, based on the analysis of the failure modes that occurred in the tests, important conclusions regarding the influence of the concrete surface preparation method used can be drawn.

Figure 6 illustrates two typical interface fracture surfaces for the case of GR and SB of concrete surface preparation. From a qualitative viewpoint, the effectiveness of the surface preparation methods used can be assessed by a visual analysis of the fracture surfaces. In the specimens where SB was used, a thicker concrete layer attached to the CFRP laminate after bond failure was found (Figure 6b). In contrast, a smaller amount of concrete attached to the CFRP surface was observed after bond failure in GR specimens (Figure 6a). In some cases, the concrete layer attached to the CFRP laminate was observed only in part of the bond length, being the remaining with neither concrete nor adhesive. This situation occurred mainly in the SB specimens with larger bond length (SB_Lb250_2, SB_Lb250_3 and SB_Lb250_4) and the reason may be related to the fact that this L_b value is higher than the theoretical effective bond length in stress transfer, promoting higher possibilities of having the influence of the existing heterogeneities in the concrete interfering with the bond conditions.

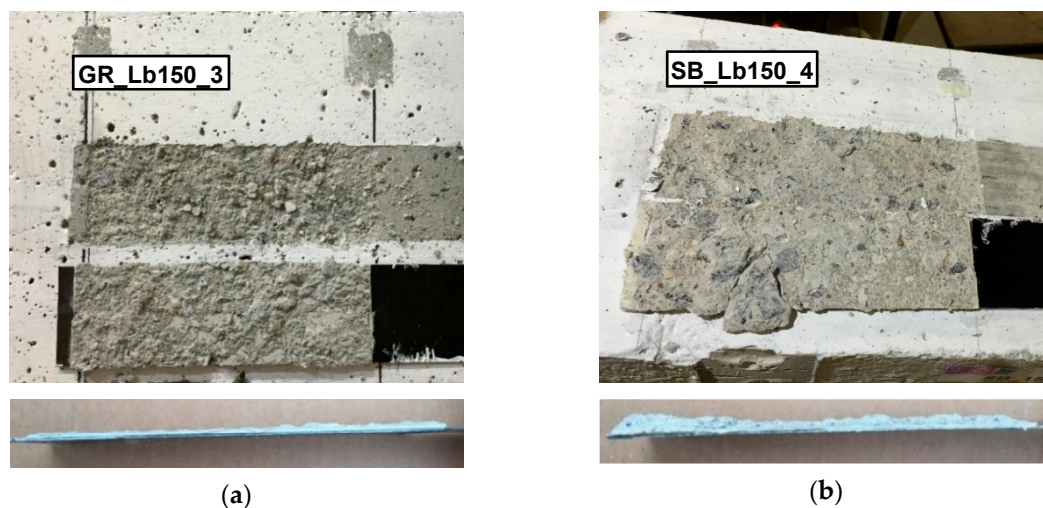


Figure 6. Fracture surface of carbon fiber reinforced polymer (CFRP)/concrete after debonding for different surface preparation methods: (a) grinding; (b) sandblasting.

Additionally, from a quantitative viewpoint, the amount of concrete attached to the CFRP after debonding failure was analyzed using a laser sensor SICK OD2-P50W10A0 with the same characteristics as the laser sensor used in the assessment of the concrete surface roughness (see Table 1 in Section 2.4). The attached layer of concrete to the CFRP laminates was measured at the middle axis along the entire bond length. In these readings, the adopted displacement rate was 0.69 mm/s and the data acquisition rate was 120 Hz, leading to consecutive readings spaced at 0.0055 mm. Figure 7a compares two representative longitudinal profiles measured by the laser sensor along the bond length of 250 mm for the case of GR and SB methods. In order to have a measurement reference, a non-adhered zone of the CFRP just before the start of the bond length (without any concrete attached) was measured, and also presented in these figures. In turn, Figure 7b shows the results in terms of average height of concrete layer attached to the CFRP, considering a constant epoxy adhesive thickness of 1 mm along the bond area. In this latter figure, the standard deviation obtained in each series is also included.

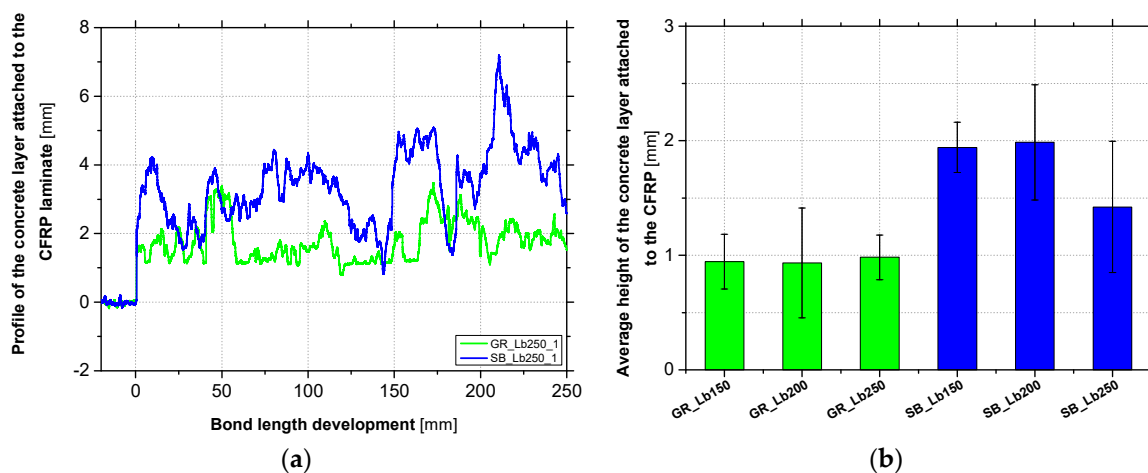


Figure 7. Concrete attached to the CFRP after debonding failure for the series Lb250 (a) and the average height of the attached concrete layer (b).

These results highlight that when SB was used, a thicker concrete layer attached to the CFRP was obtained, as had been verified in previous visual analyses of the fracture surfaces. On average, a concrete layer with a height of 1 and 1.8 mm appeared attached to the CFRP when GR and SB methods were used, respectively. As would be expected after the visual analysis of the fracture surfaces, a

higher dispersion of the average concrete layer height was observed in the CFRP laminates of the SB specimens. In fact, this surface preparation method proved to be more effective to the bond behavior and made it possible to pull some coarse aggregates out of the concrete surface. In contrast, a weaker adhesion between the concrete and the reinforcing material was verified in GR specimens.

3.3. Influence of Studied Parameters on the Bond Behavior

In this section, a more detailed analysis of the influence of the study variables on the bond behavior between concrete and EBR CFRP system is carried out. Thus, the influence of concrete surface preparation methods used (GR and SB) and the bond length adopted (150, 200 and 250 mm) on the following key aspects is investigated: (i) response in terms of pull shear force vs. loaded end slip curves (F_l-s_l), (ii) maximum shear force ($F_{l,max}$) and (iii) total energy (G_f).

3.3.1. Pull Shear Force vs. Load End Slip Curves (F_l-s_l)

Figure 8 presents the average F_l-s_l curves obtained in each test series. Each curve was obtained through the mean results of the four tests carried out under the same conditions. By the analysis of the F_l-s_l curves presented, it can be observed that the preparation method of concrete surface used did not introduce considerable changes in the strengthening system initial stiffness, since the initial branch of the curves has a practically coincident slope. However, as the debonding process of the EBR CFRP system started, higher shear force values in the case of SB specimens compared to the GR specimens were observed. Therefore, it can be concluded that the SB method proved to be more effective than GR in terms of bond strength against debonding failure.

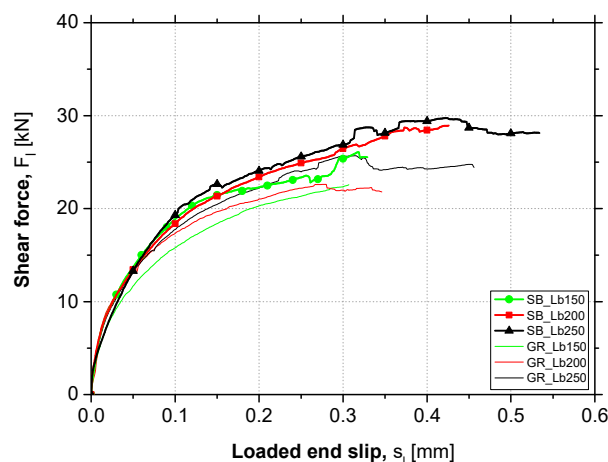


Figure 8. Average curves of the pull shear force vs. loaded end slip.

Thus, in turn, the bond length adopted did not influence the F_l-s_l curves shape neither in the linear initial branch nor in the stiffness degradation phase. Therefore, as can be seen in Figure 8 when comparing the curves with the same surface preparation method, the debonding failure process starts at very close shear force values, regardless of the L_b adopted. Nevertheless, higher values of maximum shear force and slip at the loaded end were obtained when higher L_b was used.

3.3.2. Maximum Shear Force ($F_{l,max}$)

Figure 9a shows the results obtained in terms of maximum shear force and allows to understand the influence of the concrete surface preparation method used and the bond length adopted. As expected, the SB method provided a higher bond strength between the concrete surface and the reinforcement system, with respect to the GR method. Thus, the influence of the roughness level presented by the concrete surface on the reinforcement efficiency according to the EBR technique became evident. In a more precise manner, when SB was used instead of the GR, an increase in $F_{l,max}$

of 14%, 27% and 17% was obtained on the specimens with an L_b of 150, 200 and 250 mm, respectively. In fact, the specimens with L_b of 200 mm showed a more marked increase in $F_{l,max}$ compared to the remaining test specimens. This can be explained by the fact that, in addition to the GR method being less effective than SB, the roughness level of the specimens with L_b of 200 mm was lower than the counterparts of 150 and 250 mm, as demonstrated by the lower values of R_m (see Table 2). It is also important to mention that since the concrete roughness level presents some variations, even when the same surface preparation method has been used, the influence of the bond length in the bond behavior is less significant because although it was expected to obtain higher maximum shear forces with the increase of L_b , there is inherent results variation related to the concrete surface roughness which influence the effective bond length and the corresponding maximum shear force.

Nevertheless, in relation to the influence of the adopted bond length, it is possible to identify an increase in the $F_{l,max}$ when the L_b value increases, but not in a proportional manner. This increase was more pronounced when the L_b value was changed from 150 to 200 mm, with respect to the change in L_b value from 200 to 250 mm, except for the GR specimens for the reasons explained above. Therefore, when the SB method was used, $F_{l,max}$ increases of 11% and 4% were obtained when the L_b value was changed from 150 to 200 mm and from 200 to 250 mm, respectively. These results seem to suggest that the effective anchorage length, from which an increase of L_b does not provide an increase of $F_{l,max}$, is between 200 and 250 mm, as will be proven analytically in the next sections.

3.3.3. Total Energy (G_f)

Figure 9b shows the results obtained in terms of total energy throughout the loading process until the moment that a slip of 0.3 mm was registered on the loaded end section. The analysis of these results also allows conclusions to be drawn about the effectiveness of the concrete surface preparation method used, as well as to notice the influence of the bond length adopted. According to the results, when SB was applied, the total energy dissipated until a s_l value of 0.3 mm has been registered was 14%, 10% and 3% higher than that found in the GR specimens with 150, 200 and 250 mm of L_b , respectively. Therefore, once again, the superiority of SB method in terms of reinforcement effectiveness was demonstrated when compared to the GR. This superiority would also be expected after analysis of the interface fracture surfaces (Figure 6) in which a thicker concrete layer attached to the CFRP laminate after bond failure was found in the SB specimens. This reflects the better bond behavior between CFRP and the concrete surface and justifies the higher values of G_f obtained.

In terms of the adopted bond length influence on the G_f values, increases of 6% and 10% were verified in the GR specimens when the L_b value was changed from 150 to 200 mm and from 200 to 250 mm, respectively. On the other hand, increases of 2% and 3% were observed on the SB specimens when the L_b value was changed from 150 to 200 mm and from 200 to 250 mm, respectively. In fact, the L_b value was shown to be less influential in the SB specimens, which may be justified by the fact that the total energy up to the proposed slip value is more dependent on the surface preparation method used and its effectiveness. In addition, and as mentioned in the above section, since there were inherent surface roughness variations even when the same surface preparation method was applied, the influence of the L_b value may be less significant with respect to the influence of the concrete surface roughness.

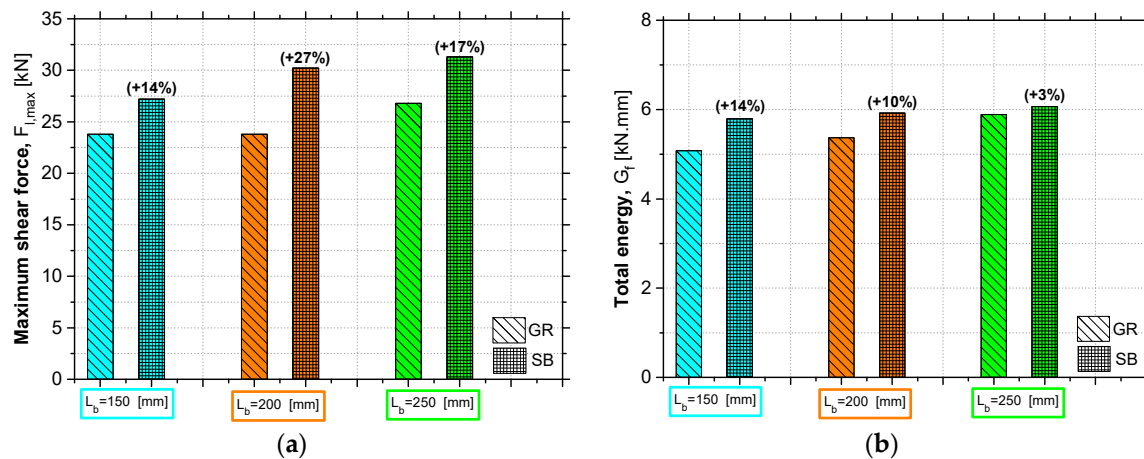


Figure 9. Influence of study parameters on the: (a) maximum pull shear force; (b) total energy. Note: the values in parentheses represents the percentage increase when SB was applied instead of GR.

3.4. Interfacial Behavior

A series of four strain gauges (SG1 to SG4) were placed along the CFRP laminate centerline to measure longitudinal strains during the loading process in the specimens with L_b of 200 mm. The analysis of longitudinal strain distribution on the CFRP surface along the bonded length allows to understand the bond behavior and debonding failure process of the strengthening system during the test.

Figure 10a,b shows the CFRP longitudinal strain distribution, at different loading levels, from the loaded end to the free end side for a bonded length of 200 mm obtained in the GR and SB specimens, respectively. The first point of each of the curves plotted (strain at loaded end section— ϵ_0) was analytically calculated by the following expression: $\epsilon_0 = F_l / (E_f \times A_f)$, where F_l , E_f and A_f represent the force applied, the CFRP Young's modulus and the CFRP cross-section area, respectively. The interface behavior presented by the GR and SB specimens was very similar due to the same failure mode occurring. Before the start of debonding process, an exponential decrease of the longitudinal strain from the loaded end section to the strain gauge installed near to the free end section (strain value close to zero) is remarkable. As soon as the debonding process starts, the longitudinal strains recorded by the SG1 (strain gauge closer to the loaded end) approximate of the strain values analytically calculated at the loaded end section, which means that the shear stresses are no longer transmitted at the interface level in this section. At this phase, the typical S-shaped strain distribution is observed and remains until the failure. The transition between these two different behaviors can be identified as the instant when the bond strength has been reached. After the debonding process has started, the strain gauges placed along the bonded length registered progressively increasing values of longitudinal strains while the shear force increased. Thus, a translation of the zone capable of stress transfer along the bonded length is observed with increasing of shear force during the debonding process.

In order to establish comparisons, Figure 10c shows the recorded strains from specimens with different concrete surface preparation methods. At the low level of applied load (10 kN), the strain profiles are very similar. However, in the SB specimen a steeper drop in the longitudinal strains was observed, which may indicate a higher initial stiffness. In the case of the highest load level concerning to the debonding process (25 kN), the influence of the concrete surface preparation method used on the interface behavior is clearer. At this same loading level, the strains recorded along the CFRP laminate of the SB specimen were significantly lower than those recorded in the GR specimen, which means a greater interface capacity in stress transfer between the CFRP and the concrete surface. Nevertheless, GR method mobilized longer bond regions in shear stress transfer. This would be expected since, due to the lower efficiency of GR method, it was necessary to mobilize a longer bond length to transfer the same amount of shear stress.

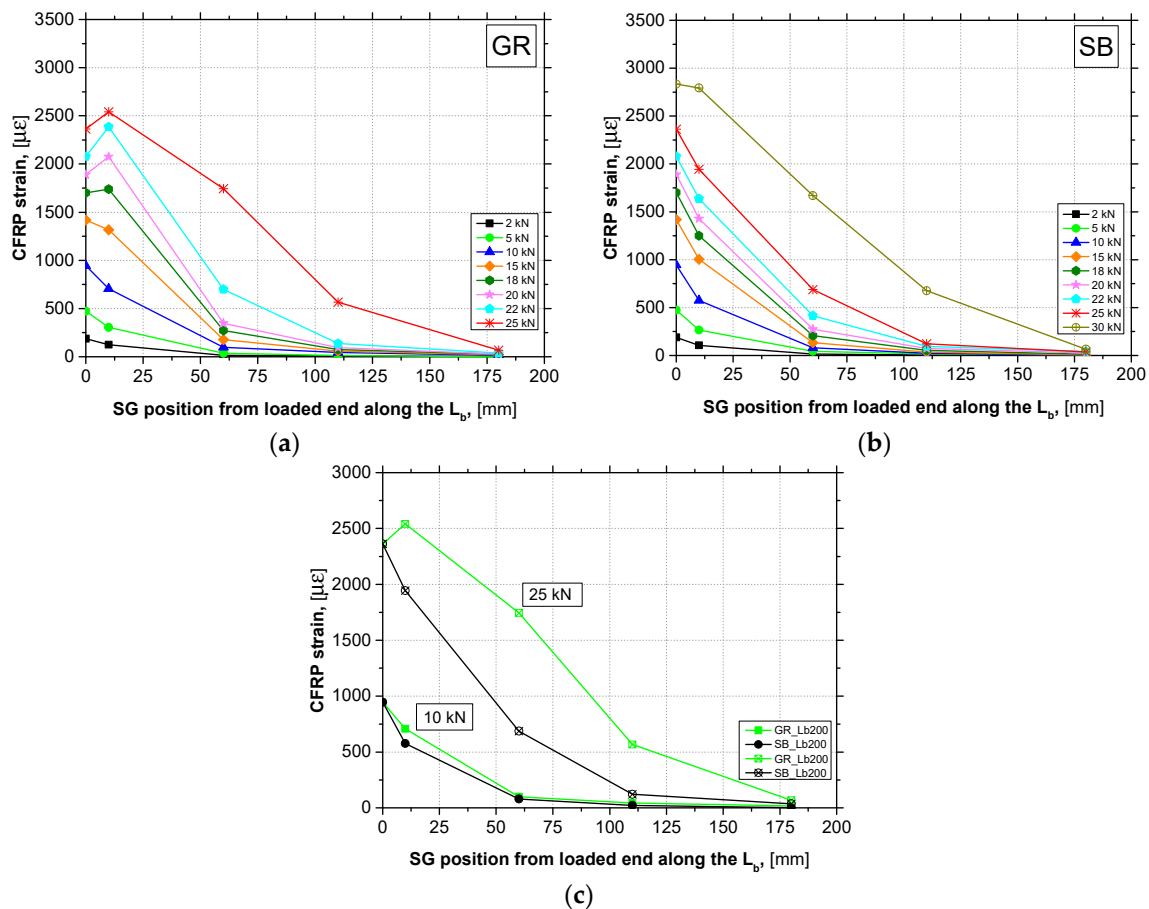


Figure 10. Longitudinal strains at different loading levels along the CFRP: (a) GR_Lb200; (b) SB_Lb200; (c) GR_Lb200 vs. SB_Lb200.

3.5. Effect of Concrete Surface Roughness on Bond Behavior—Analytical Approach

Once the influence of the concrete surface roughness on the EBR system performance was recognized, in this section the formulation proposed by the Italian guideline CNR (National Research Council) [1] for the prediction of maximum shear force of EBR FRP systems in concrete is updated/recalibrated, since the actual formula does not account for the effect of concrete surface roughness. However, this standard recognizes the importance of performing an effective surface preparation before gluing the laminate on the concrete surface. Additionally, this standard also refers that the method applied should be sandblasting and shall provide a roughness degree of at least 0.3 mm.

Figure 11a shows the relationship between the experimental maximum shear force obtained in the bond tests ($F_{l,max}$) and the mean roughness coefficient obtained in the concrete surface roughness characterization (R_m) through a linear tendency line ($R^2 = 0.8$) established as follows: $F_{l,max} = m \times R_m + b$, where m represents the effectiveness of increasing the roughness and b is the limit strength if a theoretical nil R_m value (perfectly smooth surface) could be obtained. In the formulation of the previous equation, only the results of the test series with bond length of 200 and 250 mm were included since these L_b values are not lower than the effective anchorage length (l_e) calculated according to CNR [1] (Equation (4)). According to these predictions for the concrete test specimens used in this experimental work, the l_e value from which the increase of L_b no longer means the increase of bond strength is 200 mm. It is also important to refer that the specimen SB_Lb200_3 was not included in the analytical approach presented in this section, taking into account the corresponding observed failure mode. The predicted bond strength proposed by the Italian guideline is established by Equation (5). Applying this equation for that case, the maximum shear force predicted (F_{max}) is 27.1 kN, as represented by the red

line in Figure 11a. In Equations (4) and (5), b_f , t_f and E_f are the width, thickness and Young's modulus of the CFRP material, whereas Γ_{Fm} is the fracture energy. In turn, γ_{Rd} is a corrective factor with a value of 1.25 and f_b represents the mean bond strength obtained as a function of the parameter Γ_{Fm} . The fracture energy (Γ_{Fm}) is obtained by Equation (6) where k_b is a geometrical corrective factor obtained as a function of the ratio between the width of the CFRP laminate (b_f) and the width of concrete specimen (b) (Equation (7)) and k_G is an additional experimental corrective factor which, according to CNR guideline [1], for the case of pre-cured FRP systems the average value is 0.063 mm. The parameters f_{cm} and f_{ctm} represent the average compressive and tensile strength of concrete, respectively.

$$l_e = \max \left\{ \frac{1}{\gamma_{Rd} \cdot f_b} \sqrt{\frac{\pi^2 \cdot E_f \cdot t_f \cdot \Gamma_{Fm}}{2}}, 200 \text{ mm} \right\}, \quad (4)$$

$$F_{max} = b_f \cdot \sqrt{2 \cdot E_f \cdot t_f \cdot \Gamma_{Fm}}, \quad (5)$$

$$\Gamma_{Fm} = k_b \cdot k_G \cdot \sqrt{f_{cm} \cdot f_{ctm}}, \quad (6)$$

$$k_b = \sqrt{\frac{2 - b_f/b}{1 + b_f/b}} \geq 1 \quad \text{if} \quad b_f/b \geq 0.25. \quad (7)$$

Analyzing Figure 11a, it is remarkable that the formulation presented by the CNR [1] can be considered as a good prediction of bond strength when the concrete surface preparation method used has a limited efficiency. By comparing the prediction of F_{max} provided by the guideline with the experimental values of maximum shear force obtained in SB specimens, it is clear that improvements in the formulation are needed.

Therefore, in order to improve the analytical formulation taking into account the influence of the concrete surface roughness prior to the EBR system installation and allow a better prediction of the bond strength when a more effective surface preparation method is used, the following procedure was adopted: (i) using the Equation (5) and considering the value F_{max} equal to the maximum shear force obtained from experimental tests, the average experimental values of Γ_{Fm} were calculated; then, (ii) using the values of Γ_{Fm} inside Equation (6) and all the other known parameters, the experimental values of k_G were obtained. Figure 11b shows the relation between the experimental k_G values and the mean roughness coefficient obtained in the concrete surface roughness characterization (R_m) through a linear tendency line ($R^2 = 0.8$). In the same figure, the k_G value proposed by the Italian guideline is represented by a red line. As concluded by the accuracy of the maximum shear force prediction, it is also verified that the k_G mean value suggested by the CNR [1] can accurately predict the experimental values obtained when the concrete surface preparation method adopted does not provide high levels of roughness. The same observation cannot be drawn when a more effective surface preparation method is used. In the SB specimens, the k_G value obtained proved to be higher than that suggested by the formulation included in the CNR guideline.

To improve the F_{max} prediction (Equation (5)) maintaining the k_G value suggested by the guideline, a new parameter (k_R —roughness corrective factor) was introduced in the calculation of the average interface fracture energy (Γ_{Fm}), which is defined as a function of the mean roughness coefficient (R_m), as demonstrated by Equations (8) and (9). From GR to SB, values of k_R ranged between 0.8 and 1.7, respectively. According to the obtained results, the CNR guideline [1] considers in its formulation ($k_R = 1$) a surface preparation method slightly more effective than the GR ($k_R = 0.9$, in average terms) and markedly less effective than the SB ($k_R = 1.4$, in average terms). In the absence of any information about the concrete surface roughness, it is recommended to use a value of k_R equal to 1, as suggested in the CNR standard.

In order to assess the accuracy of the proposed analytical formulation, the average values of maximum shear force for each test series, obtained from the analytical model and from the experimental tests are compared with the prediction provided by the CNR guideline [1] in Figure 12a. The values of maximum shear force for each specimen, obtained from the analytical model and from the experimental

tests are also compared in Figure 12b. From these figures, it is possible to verify the high accuracy of the proposed analytical model. The difference between analytical and experimental results was determined by Equation (10). Through the inclusion of the roughness corrective factor (k_R) on existing CNR formulation for predicting the F_{max} , the error values between the analytical formulation results and the experimental results were reduced from 11.8% to 4.4%.

$$k_R = \frac{0.09R_m + 0.04}{0.063} = 1.4 R_m + 0.7, \tag{8}$$

$$\Gamma_{Fm} = k_b \cdot k_G \cdot k_R \sqrt{f_{cm} \cdot f_{ctm}}, \tag{9}$$

$$\% \text{ RPE} = \frac{|F_{l,max,exp} - F_{l,max,anal}|}{F_{l,max,exp}} \times 100. \tag{10}$$

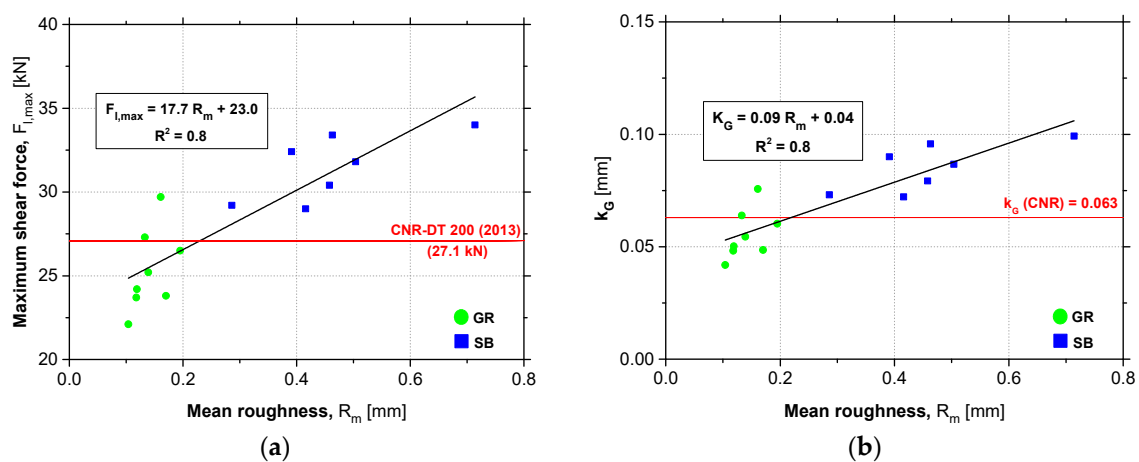


Figure 11. Relationship between the following parameters: (a) $F_{l,max}$ vs. R_m ; (b) k_G vs. R_m .

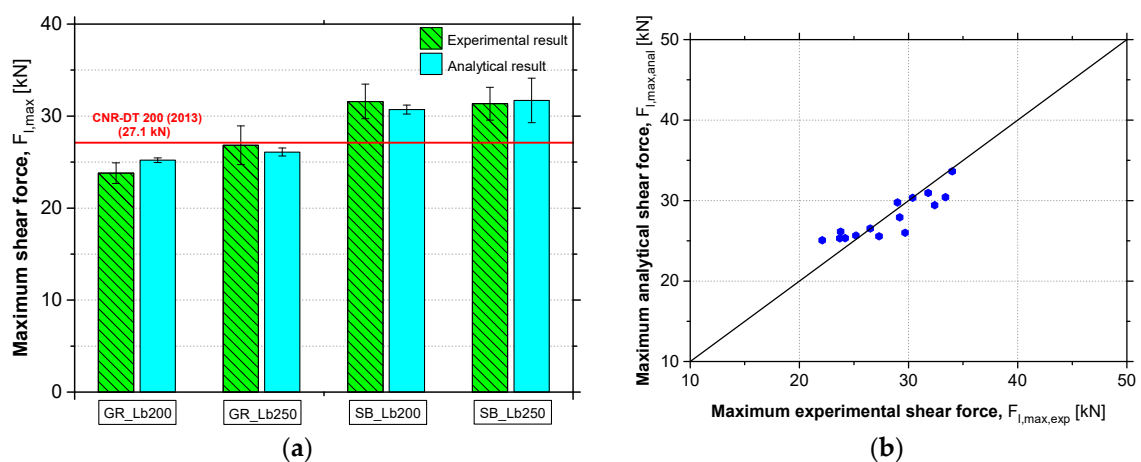


Figure 12. Comparison between the experimental results, the analytical results and the prediction provided by National Research Council [1] (a) and the accuracy of the proposed analytical model (b).

4. Conclusions

This paper presented and analyzed the obtained results from an experimental program composed of 24 single-lap shear tests in prismatic concrete specimens with CFRP laminates applied according to the EBR technique. The aim of this work was to study the influence of some important parameters on the bond behavior between concrete and the CFRP laminate, namely: (i) the type of concrete surface

preparation method used before the application of EBR system that provides different levels of surface roughness (GR—grinding and SB—sandblasting) and (ii) the bond length (150, 200 and 250 mm). For this purpose, the roughness of the distinct concrete surfaces was assessed by using a laser sensor in order to allow the identification of its influence on the bond strength. Additionally, the formulation proposed by the Italian guideline CNR [1] for the prediction of maximum shear force of EBR FRP systems in concrete was updated/recalibrated, since the actual formulation does not account for the effect of concrete surface roughness. Thus, the following main conclusions can be highlighted:

- Based on the measurements performed with the laser sensor, the results clearly showed that the SB method produced a higher level of concrete surface roughness than the GR. In terms of mean roughness coefficient (R_m) and the root mean square (R_q), the SB method yielded to an average increase of 250% and 150%, respectively, in relation to the surface preparation with GR;
- Different roughness levels, provided by the different preparation methods of the concrete surface, resulted in different levels of bond strength;
- Cohesive debonding in the concrete was the governed failure mode observed in all tests carried out, regardless of the surface preparation method used and bond length adopted. After debonding failure, a concrete layer attached to the epoxy adhesive and CFRP laminate was observed. In SB specimens, this concrete layer was considerably thicker than the layer observed in GR specimens, which reflects the better bond behavior provided by the SB method;
- The analysis of the F_l-s_l curves allowed to verify that the different preparation methods of the concrete surface did not significantly change the initial stiffness of the strengthening system. However, the debonding process started at higher shear force values in the case of SB specimens compared to the GR specimens. Thus, in turn, the increase of L_b value did not influence the F_l-s_l curves shape neither in the initial branch nor in the stiffness degradation phase and the debonding process;
- The use of the SB method instead of GR provided an increase of maximum shear force ($F_{l,max}$) and total energy (G_f), allowing a better use of the tensile strength capacity of the CFRP laminate;
- The use of higher L_b values provided an increase of maximum shear force ($F_{l,max}$) and total energy (G_f);
- Based on the obtained results from the experimental program, the influence of the surface roughness was included in the analytical formulation for predicting the maximum shear force proposed by CNR [1], through the inclusion of the roughness corrective factor (k_R) defined as a function of the mean roughness coefficient (R_m). The proposed analytical model proved to be able to accurately predict the bond strength of the EBR FRP system taking into account the roughness level of the concrete surface where the CFRP laminate is subsequently installed.

Author Contributions: Conceptualization, validation and formal analysis, S.S. and J.S.-C.; methodology and investigation, S.S., J.S.-C., J.R.C. and P.F.; writing—original draft preparation, S.S.; writing—review and editing, S.S., J.S.-C., J.R.C.; supervision, J.S.-C.; funding acquisition, J.S.-C.

Funding: This work was carried out in scope of the project FRPLongDur POCI-01-0145-FEDER-016900 (FCT PTDC/ECM-EST/1282/2014) funded by national funds through the Foundation for Science and Technology (FCT) and co-financed by the European Fund of the Regional Development (FEDER) through the Operational Program for Competitiveness and Internationalization (POCI) and the Lisbon Regional Operational Program and, partially financed by the project POCI-01-0145-FEDER-007633.

Acknowledgments: The authors also like to thank the S&P Clever Reinforcement Ibérica Lda. company for providing the materials. The first author wishes also to acknowledge the grant SFRH/BD/131913/2017 provided by FCT.

Conflicts of Interest: The authors declare no conflict of interest.

References

1. Council, N.R. *Guide for the Design and Construction of Externally Bonded FRP Systems for Strengthening Existing Structures*; CNR-DT 200R1; Advisory Committee on Technical Recommendations for Construction: Rome, Italy, 2013.
2. Fédération Internationale Du Béton. Design and use of externally bonded FRP reinforcement for RC structures. *Bulletin* **2001**, *14*.
3. Bank, L.C. *Composites for Construction: Structural Design with FRP Materials*; John Wiley & Sons: Hoboken, NJ, USA, 2006. [[CrossRef](#)]
4. Sena-Cruz, J.M.; Barros, J.A.; Coelho, M.R.; Silva, L.F. Efficiency of different techniques in flexural strengthening of RC beams under monotonic and fatigue loading. *Constr. Build. Mater.* **2012**, *29*, 175–182. [[CrossRef](#)]
5. Bakis, C.E.; Bank, L.C.; Brown, V.; Cosenza, E.; Davalos, J.; Lesko, J.; Machida, A.; Rizkalla, S.; Triantafillou, T. Fiber-reinforced polymer composites for construction—State-of-the-art review. *J. Compos. Constr.* **2002**, *6*, 73–87. [[CrossRef](#)]
6. Kaiser, H. Bewehren von Stahlbeton Mit Kohlenstoffaserverstärkten Epoxidharzen. Doctoral Thesis, Eidgenössischen Technischen Hochschule (ETH), Zürich, Switzerland, 1989.
7. Czaderski, C.; Meier, U. EBR Strengthening Technique for Concrete, Long-Term Behaviour and Historical Survey. *Polymers* **2018**, *10*, 77. [[CrossRef](#)]
8. Chen, J.F.; Teng, J.G. Anchorage strength models for FRP and steel plates bonded to concrete. *J. Struct. Eng.* **2001**, *127*, 784–791. [[CrossRef](#)]
9. Ceroni, F.; Pecce, M.; Matthys, S.; Taerwe, L. Debonding strength and anchorage devices for reinforced concrete elements strengthened with FRP sheets. *Compos. Part B Eng.* **2008**, *39*, 429–441. [[CrossRef](#)]
10. Ceroni, F.; Pecce, M. Evaluation of bond strength in concrete elements externally reinforced with CFRP sheets and anchoring devices. *J. Compos. Constr.* **2010**, *14*, 521–530. [[CrossRef](#)]
11. Iovinella, I.; Prota, A.; Mazzotti, C. Influence of surface roughness on the bond of FRP laminates to concrete. *Constr. Build. Mater.* **2013**, *40*, 533–542. [[CrossRef](#)]
12. Savoia, M.; Mazzotti, C.; Ferracuti, B. Mode II fracture energy and interface law for FRP concrete bonding with different concrete surface preparations. In Proceedings of the FRAMCOS-6 Conference, Catania, IT, USA, 17–22 June 2007.
13. Bilotta, A.; Ceroni, F.; Di Ludovico, M.; Nigro, E.; Pecce, M.; Manfredi, G. Bond efficiency of EBR and NSM FRP systems for strengthening concrete members. *J. Compos. Constr.* **2011**, *15*, 757–772. [[CrossRef](#)]
14. Ali-Ahmad, M.; Subramaniam, K.; Ghosn, M. Experimental investigation and fracture analysis of debonding between concrete and FRP sheets. *J. Eng. Mech.* **2006**, *132*, 914–923. [[CrossRef](#)]
15. Mazzotti, C.; Bilotta, A.; Carloni, C.; Ceroni, F.; D’Antino, T.; Nigro, E.; Pellegrino, C. Bond between EBR FRP and concrete. In *Design Procedures for the Use of Composites in Strengthening of Reinforced Concrete Structures*; Springer: Dordrecht, The Netherlands, 2016; pp. 39–96. [[CrossRef](#)]
16. Seracino, R.; Raizal Saifulnaz, M.R.; Oehlers, D.J. Generic debonding resistance of EB and NSM plate-to-concrete joints. *J. Compos. Constr.* **2007**, *11*, 62–70. [[CrossRef](#)]
17. Mazzotti, C.; Savoia, M.; Ferracuti, B. A new single-shear set-up for stable debonding of FRP-concrete joints. *Constr. Build. Mater.* **2009**, *23*, 1529–1537. [[CrossRef](#)]
18. Yao, J.; Teng, J.G.; Chen, J.F. Experimental study on FRP-to-concrete bonded joints. *Compos. Part B Eng.* **2005**, *36*, 99–113. [[CrossRef](#)]
19. Chajes, M.J.; Finch, W.W., Jr.; Januszka, T.F.; Thomson, T.A., Jr. Bond and force transfer of composite material plates bonded to concrete. *ACI Struct. J.* **1996**, *93*, 208–217.
20. Sena-Cruz, J.M.; Barros, J.A.O. Bond between near-surface mounted carbon-fiber-reinforced polymer laminate strips and concrete. *J. Compos. Constr.* **2004**, *8*, 519–527. [[CrossRef](#)]
21. Fernandes, P.M.G.; Silva, P.M.; Sena-Cruz, J. Bond and flexural behavior of concrete elements strengthened with NSM CFRP laminate strips under fatigue loading. *Eng. Struct.* **2015**, *84*, 350–361. [[CrossRef](#)]
22. De Lorenzis, L.; Teng, J.G. Near-surface mounted FRP reinforcement: An emerging technique for strengthening structures. *Compos. Part B Eng.* **2007**, *38*, 119–143. [[CrossRef](#)]
23. Coelho, M.R.F.; Sena-Cruz, J.M.; Neves, L.A.C. A review on the bond behavior of FRP NSM systems in concrete. *Constr. Build. Mater.* **2015**, *93*, 1157–1169. [[CrossRef](#)]

24. De Lorenzis, L.; Rizzo, A.; La Tegola, A. A modified pull-out test for bond of near-surface mounted FRP rods in concrete. *Compos. Part B Eng.* **2002**, *33*, 589–603. [[CrossRef](#)]
25. Coelho, M.R.F.; Fernandes, P.M.G.; Sena-Cruz, J.; Barros, J.A. Bond between multidirectional laminates of CFRP and concrete. In Proceedings of the 6th International Conference on FRP Composites in Civil Engineering–CICE2012, Rome, Italy, 13–15 June 2012.
26. Nardone, F.; Lignola, G.P.; Prota, A.; Manfredi, G.; Nanni, A. Modeling of flexural behavior of RC beams strengthened with mechanically fastened FRP strips. *Compos. Struct.* **2011**, *93*, 1973–1985. [[CrossRef](#)]
27. Lee, J.H.; Lopez, M.M.; Bakis, C.E. Slip effects in reinforced concrete beams with mechanically fastened FRP strip. *Cem. Concr. Compos.* **2009**, *31*, 496–504. [[CrossRef](#)]
28. Elsayed, W.E.; Ebead, U.A.; Neale, K.W. Studies on mechanically fastened fiber-reinforced polymer strengthening systems. *ACI Struct. J.* **2009**, *106*, 49.
29. Bank, L.C.; Arora, D. Analysis of RC beams strengthened with mechanically fastened FRP (MF-FRP) strips. *Compos. Struct.* **2007**, *79*, 180–191. [[CrossRef](#)]
30. ICRI. Technical Guideline 03732—Selecting and Specifying Concrete Surface Preparation for Sealers. In *Coatings, and Polymers Overlays*; International Concrete Repair Institute: Des Plaines, IL, USA, 1997.
31. American Concrete Institute (ACI). *Design and Construction of Externally Bonded FRP Systems for Strengthening Concrete Structures*; ACI 440.2R-02; American Concrete Institute: Farmington Hills, MI, USA, 2002.
32. Galecki, G.; Maerz, N.; Nanni, A.; Myers, J. Limitations to the use of waterjets in concrete substrate preparation. In Proceedings of the Annual American Waterjet Conference, Minneapolis, MN, USA, 18–21 August 2001; pp. 483–493.
33. Correia, L.; Teixeira, T.; Michels, J.; Almeida, J.A.P.P.; Sena-Cruz, J. Flexural behaviour of RC slabs strengthened with prestressed CFRP strips using different anchorage systems. *Compos. Part B Eng.* **2015**, *81*, 158–170. [[CrossRef](#)]
34. NP EN 12390-13. *Testing Hardened Concrete. Part 13: Determination of Secant Modulus of Elasticity in Compression*; Instituto Português da Qualidade (IPO): Caparica, Portugal, 2014.
35. NP EN 12390-3. *Testing Hardened Concrete. Part 3: Compressive Strength of Test Specimen*; Instituto Português da Qualidade (IPO): Caparica, Portugal, 2011.
36. ISO 527-5. *Plastics—Determination of Tensile Properties. Part 5: Test Conditions for Unidirectional Fibre-Reinforced Plastic Composites*; International Organization for Standardization (ISO): Genève, Switzerland, 2009.
37. ISO 527-2. *Plastics—Determination of Tensile Properties. Part 2: Test Conditions for Moulding and Extrusion Plastics*; International Organization for Standardization (ISO): Genève, Switzerland, 2012.



© 2019 by the authors. Licensee MDPI, Basel, Switzerland. This article is an open access article distributed under the terms and conditions of the Creative Commons Attribution (CC BY) license (<http://creativecommons.org/licenses/by/4.0/>).